Supplementary Fig. 1

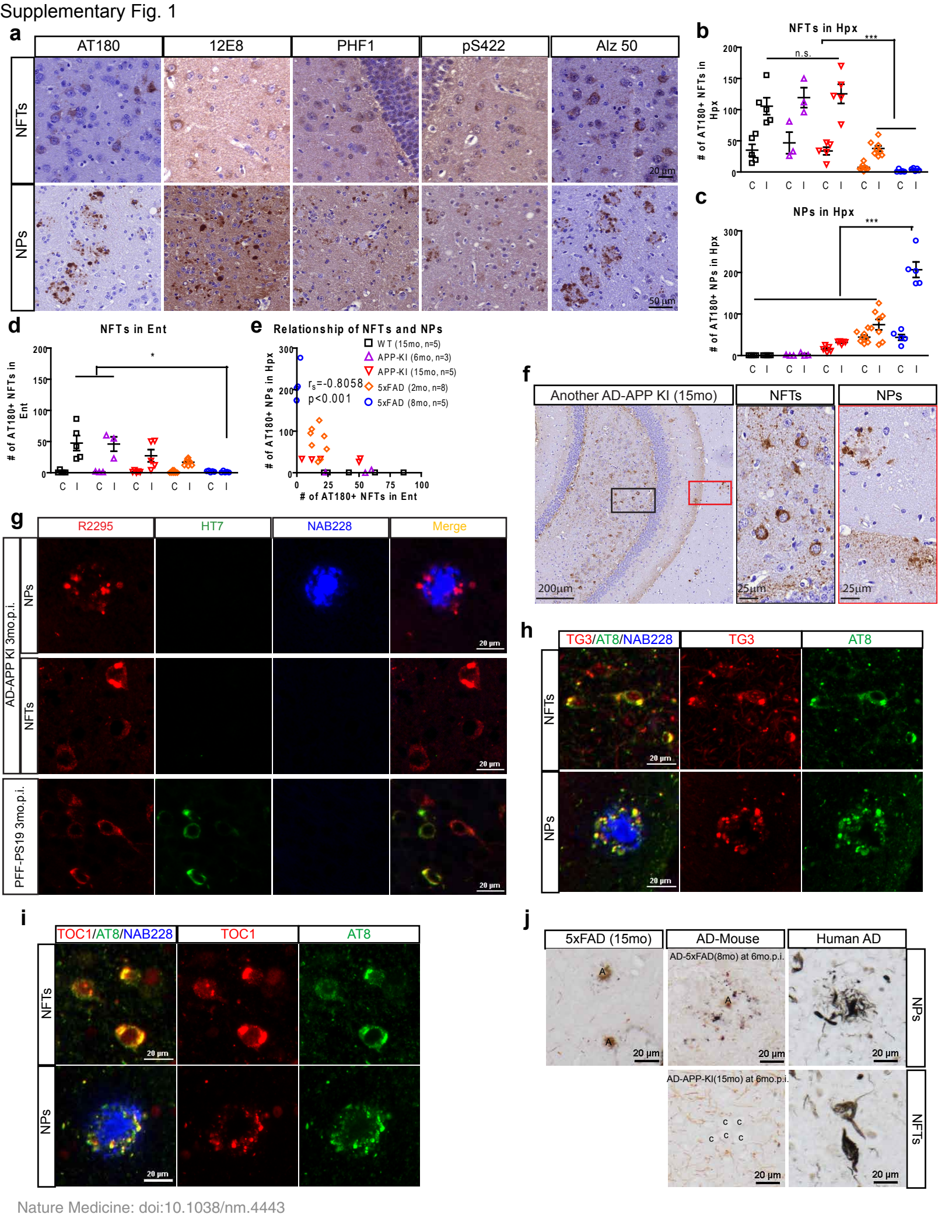

Supplementary Figure 1: Characterization of NPs and NFTs induced by AD-tau.

a, Representative immunohistochemistry staining of the induced NFTs and NPs at 3 mo.p.i. of AD-tau detected with anti-tau antibodies with different epitopes: AT180 (pThr231), 12E8 (pSer262/pSer356), PHF1(pSer396/pSer404), pS422 (pSer422), Alz50 (misfolded conformation of AD-tau). Quantification of AT180-positive NFTs (**b**) and NPs (**c**) in hippocampus; and NFTs (**d**) in entorhinal cortex for both ipsilateral (I) and contralateral (C) sides of the WT, APP-KI and 5xFAD mice injected with AD-tau and analyzed at 3 mo.p.i.. Color codes are in **e**. One-way ANOVA with Tukey's multiple comparison tests were performed, $^{**}P < 0.01$, $^{***}P < 0.001$. **e,** inverse correlation between AT180+ NPs in the ipsilateral hippocampus and AT180+ NFTs in the ipsilateral entorhinal cortex (Spearman correlation $r_s = -0.806$, $p<0.001$). **f**, The induction of AD-like NFT and NP tau pathologies are not case-specific. 15-month old APP KI mice injected with AD-tau purified from a second AD brain also showed AD-like AT8+ NFTs and NPs at 3 mo.p.i.. Right panels are the higher magnification of the areas within the rectangles on the left. The black frame shows magnified views of the AD-like NFTs and the red frame shows magnified views of NPs. **g**, Triple-labeling with rabbit anti-mouse tau-selective antibody R2295, human tau-selective MAb HT7 and Aβ antibody NAB228 in AD-APP KI (15mo). Tau PFF-injected PS19 mice overexpressing human tau with a P301S *MAPT* mutation (PFF-PS19) at 3mo.p.i. is used as a positive control for HT7 antibody. Triple labeling of NFTs and NPs with AT8, Aβ plaques with NAB228 and **h,** conformation-dependent anti-tau antibody TG3 or **i,** oligomeric anti-tau antibody TOC1 in APP-KI (15 mo) at 3 mo.p.i. **j**, Gallyas silver staining of the NFTs and NPs. Right column, the positive silver staining of both NPs and NFTs in human AD brain sections. Middle columns, the silver staining on AD-5xFAD (8mo) or AD-APP-KI (15mo) at 6 mo.p.i. with AT8-positive NPs or AD-like NFTs, respectively. Only NP tau showed appreciable silver staining in the AD-tau-injected 5xFAD mice, while no Gallyas positive AD-like NFT-tau can be detected up to 6 mo.p.i. Left column, similarly aged non-injected 5xFAD mice (15mo) showed minimal silver staining of neurites around Aβ plaques. Black signal indicates the real silver staining. Letter A denotes Aβ plaque core and letter C denotes neuronal cell body.

Supplementary Fig. 2

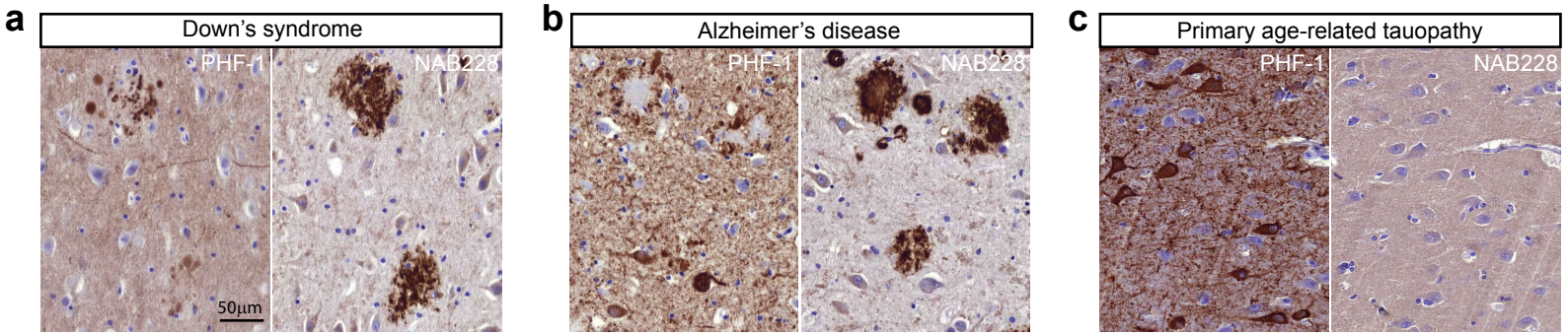

Supplementary Figure 2: The relationship between NPs and NFTs in human disease.

Representative immunostaining with MAbs PHF-1 and NAB228 on pairs of adjacent brain sections from **a,** 4 cases of young Down's syndrome patients with Aβ plaque pathology and NPs, **b,** 9 cases of AD with Aβ plaques and both NPs and NFTs, **c,** 7 cases of primary age-related tauopathy patients with NFTs.

Nature Medicine: doi:10.1038/nm.4443

Supplementary Fig. 3

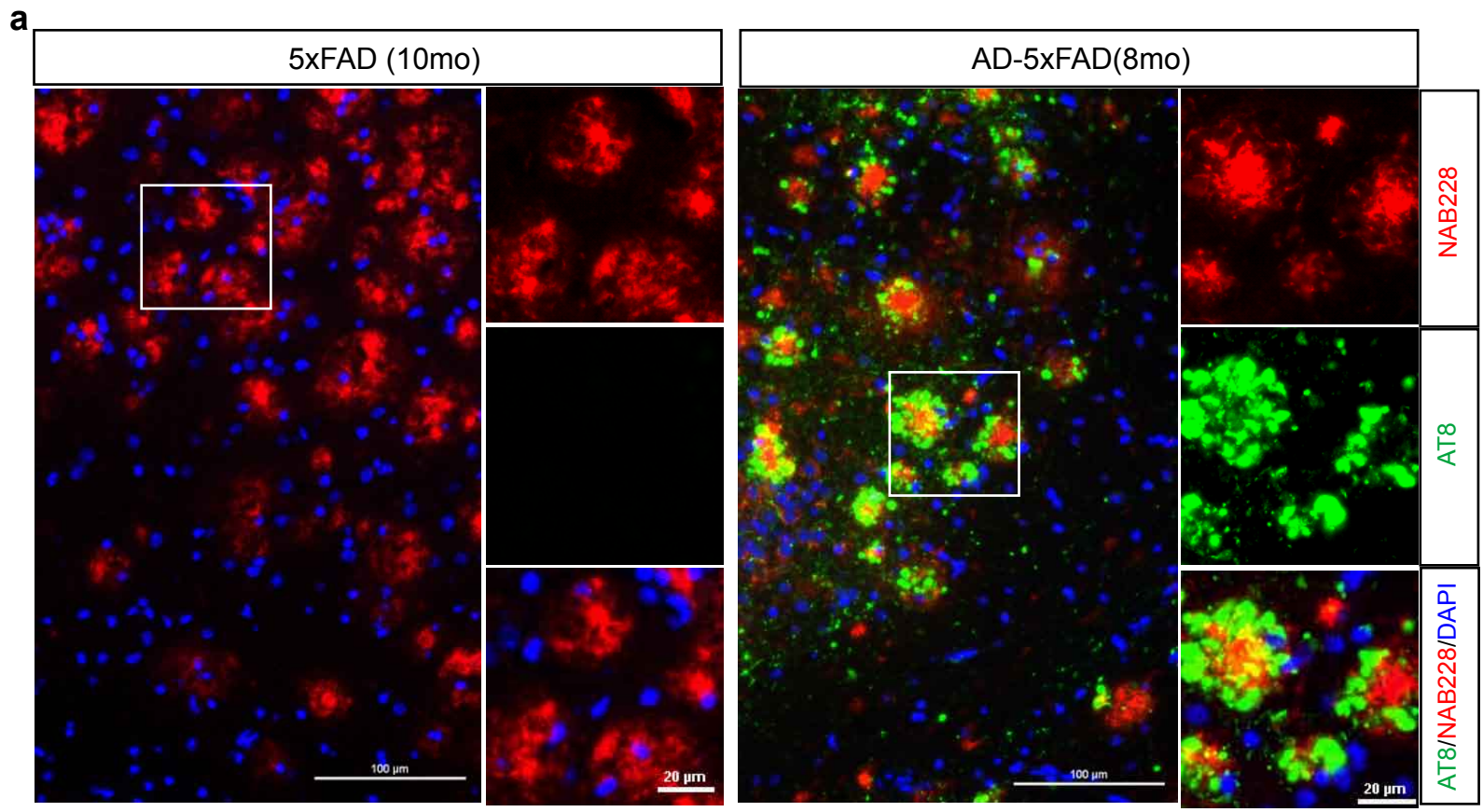

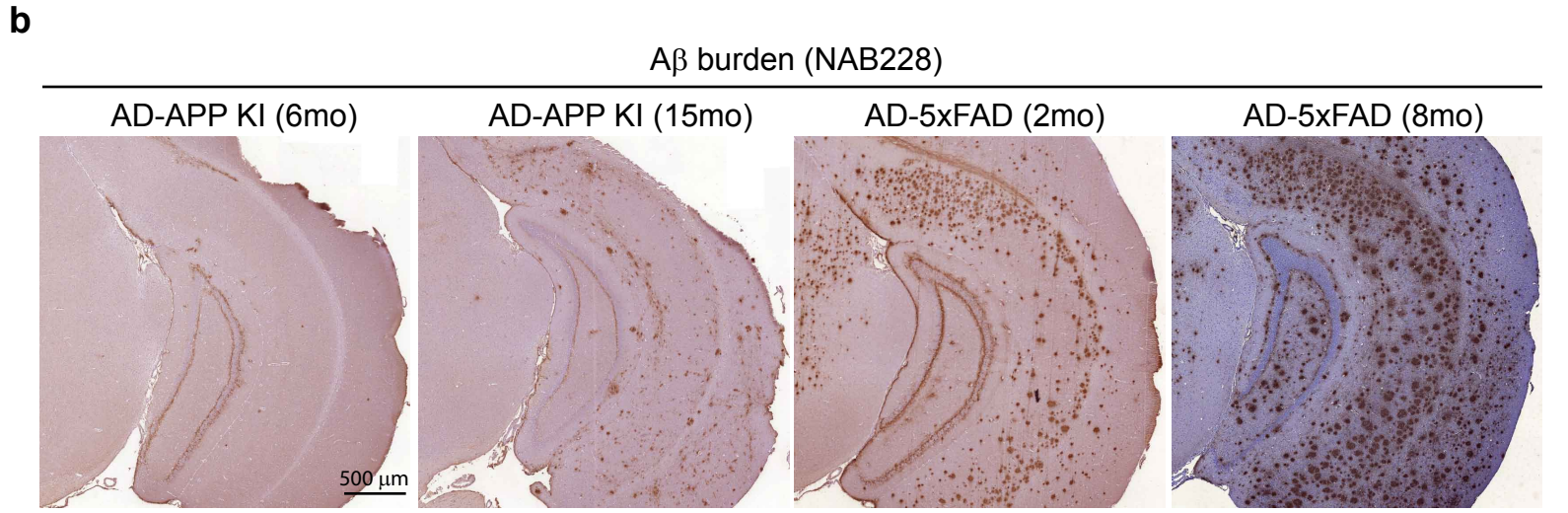

Supplementary Figure 3: The Aβ plaque burden positively correlates with the induction of NPs.

a, Double labeling with AT8 and NAB228 antibodies in 5xFAD (8mo) mice without or with AD-tau injection at 3 mo.p.i.. Areas within the square frames are shown in the panels on the right at higher magnifications. **b,** Representative immunostaining with NAB228 antibody showing the Aβ burden in APP-KI and 5xFAD mice at different ages injected with the same dose of AD-tau at 3 mo.p.i.. AD-APP-KI (6mo, n=3), AD-APP-KI (15mo, n=5), AD-5xFAD (2mo, n=8) and AD-5xFAD (8mo, n=5) were quantified and the quantifications of the Aβ burden are shown in Figure 1q.

Supplementary Fig. 4

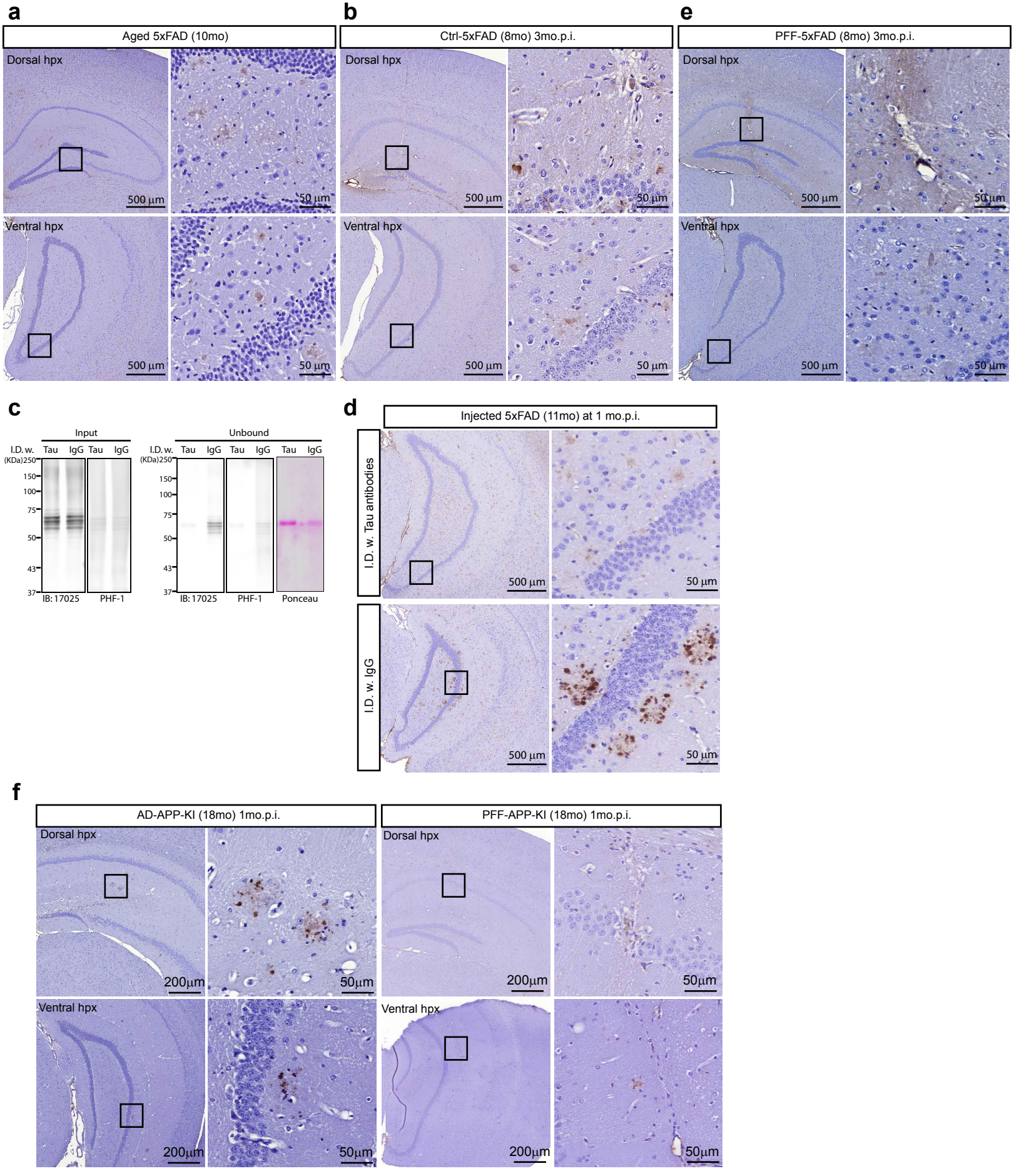

Supplementary Figure 4: AD-tau, but not synthetic tau fibrils, induces NPs in old 5xFAD mice.

Representative AT8 immunostaining of ipsilateral dorsal (top) and ventral (bottom) hippocampal regions from **a,** 5xFAD (10mo) mice; **b,** 5xFAD (8mo) mice injected with control brain lysate at 3 mo.p.i. and **e,** 5xFAD (8mo) mice injected with 4.5 µg tau PFFs assembled from recombinant tau proteins at 3 mo.p.i.. None showed convincing AT8+ tau pathologies at the indicated time points. **c,** AD brain lysates containing the same amount of AD-tau proteins were respectively incubated with anti-tau antibodies or IgG control, and the immunoblot shows that AD-tau was largely immuno-depleted (I.D.) from the AD brain lysates, while the main protein contaminants detected by Ponceau red were still present. **d,** Representative AT8 immunostaining of ipsilateral ventral hippocampus for 5xFAD (11mo) mice injected with AD brain lysates immuno-depleted with (top) or without (bottom) anti-tau antibodies at 1 mo.p.i.. **f,** Representative AT8 immunostaining of ipsilateral dorsal and ventral hippocampus in APP-KI (18mo) mice injected with 2 µg AD-tau or 4.5 µg tau PFFs assembled from recombinant tau proteins at 1 mo.p.i.. The images on right panels in **a, b, d, e, f** are higher magnifications of the areas within black squares on the left. Each group contains 3 mouse.

Supplementary Fig. 5

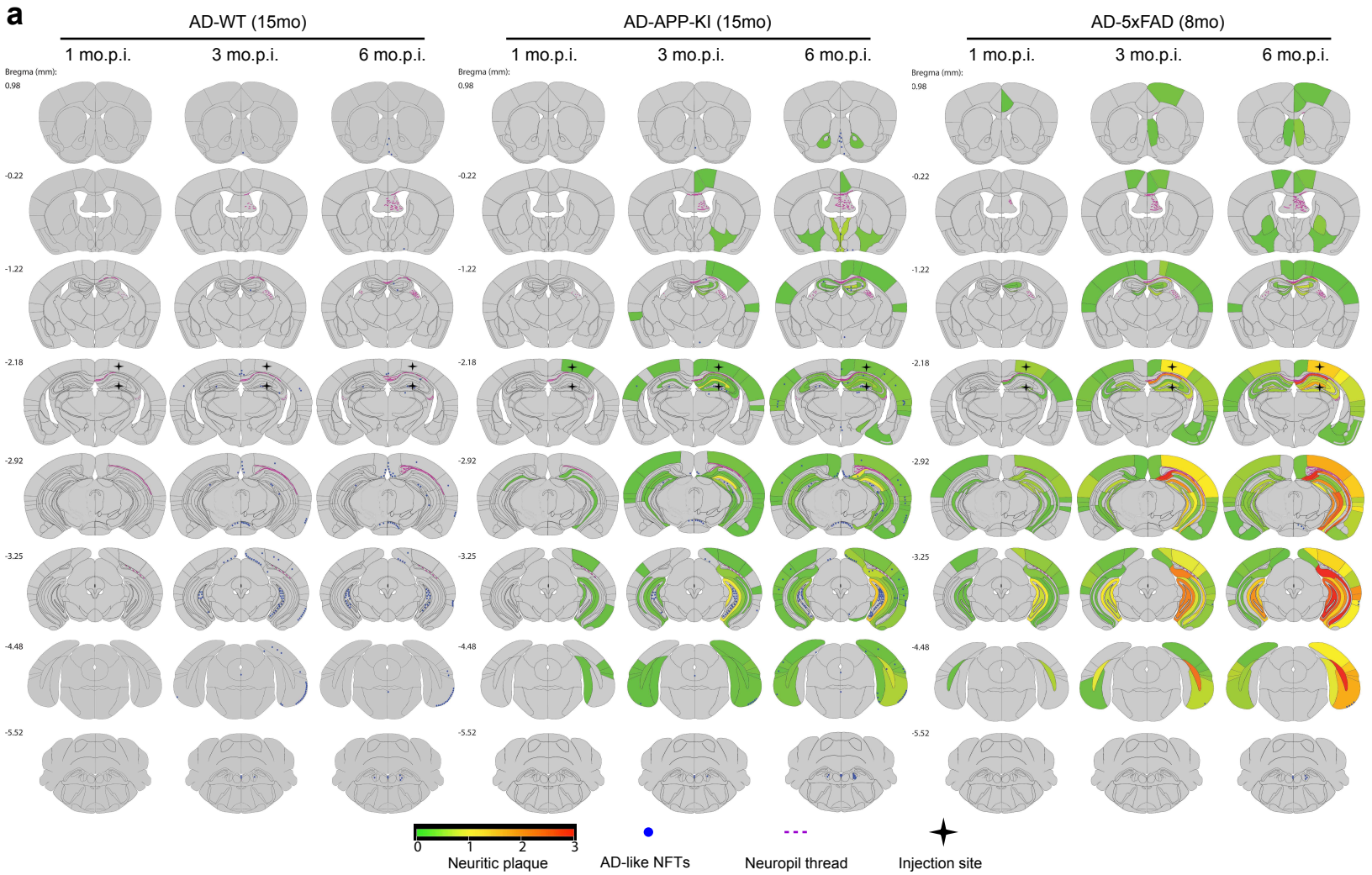

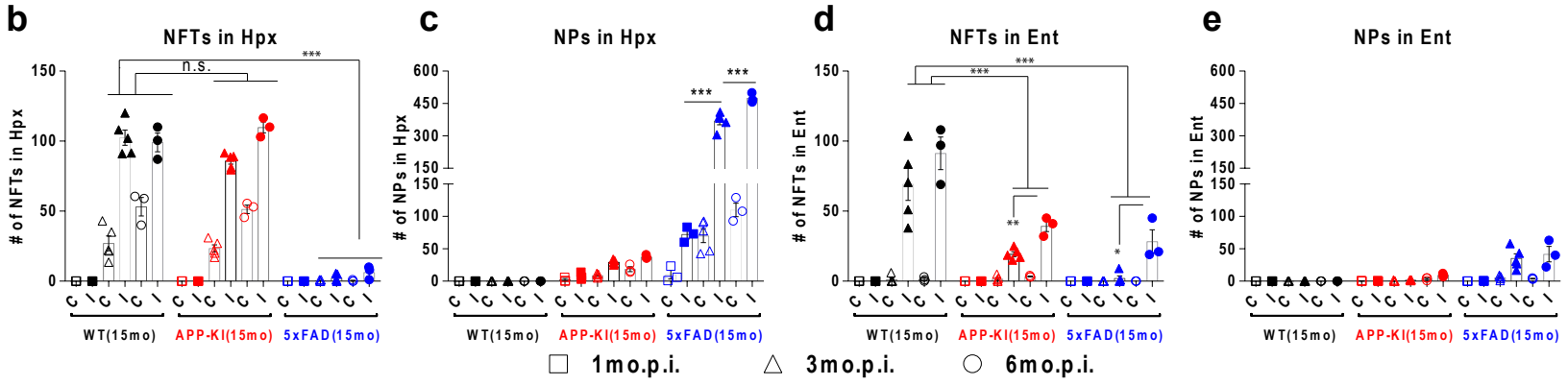

Nature Medicine: doi:10.1038/nm.4443

Supplementary Figure 5: Time course of dynamic changes of tau in AD-like NFTs and NPs in vivo.

a, Heatmaps representing the semi-quantitative analysis of AD-like NFTs and NPs based on AT8 immunostaining in AD-tau injected WT (15mo), APP-KI (15mo) and 5xFAD (8mo) mice at 1-, 3- and 6 mo.p.i.. Coronal planes at Bregma (mm) 0.98, -0.22, -1.22, -2.18, -2.92, -3.25, -4.48 and -5.52 are shown. Heat colors represent tau positive NPs (0: no pathology, gray; 3: maximum pathology, red), blue dots represent tau positive AD-like NFTs, purple lines represent tau positive NTs in the corpus callosum and fimbria. Black stars indicate the injection sites. Average scores from each cohort mice are presented. The number of NFTs (**b**) and NPs (**c)** in hippocampus (Hpx), and NFTs (**d**) and NPs (**e**) in entorhinal cortex (ENT) were quantified temporally in both ipsilateral (I) and contralateral (C) sides in each cohort shown in **a.** Each group contains 3-5 mice, each indicated as a dot in the graphs **b-e**. Data are presented with the mean ± s.e.m., and one-way ANOVAs with Tukey's tests, $^{**}P \leq 0.01$, $^{***}P \leq 0.001$.

Supplementary Fig. 6

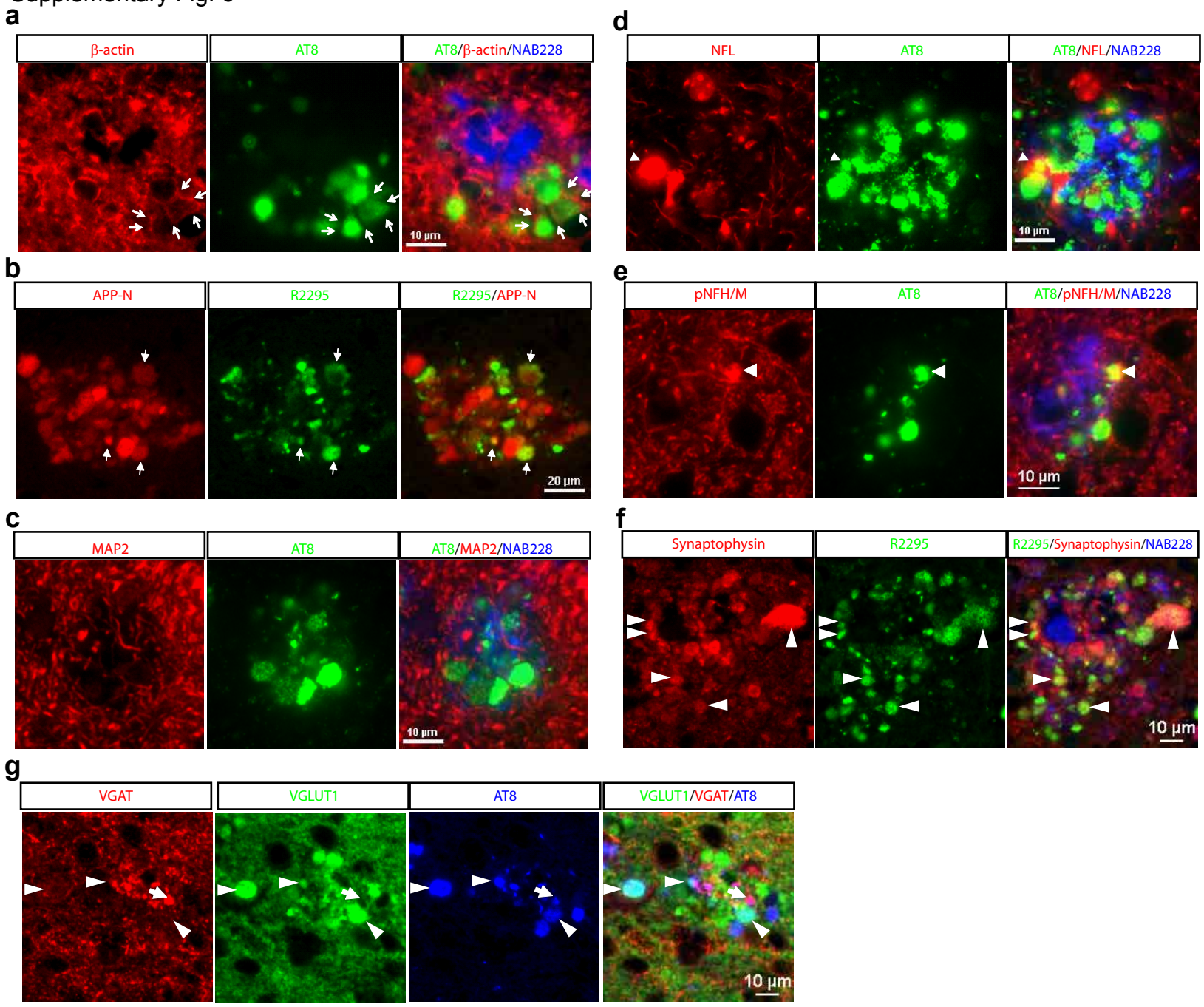

Supplementary Figure 6: Subcellular localization of NP tau pathologies.

a, Triple-labeling of NPs with antibodies AT8, NAB228 and β-actin, showing tau positive NPs are surrounded by β-actin enriched membrane boundaries. Arrows indicate the β-actin boundaries. **b,** double-labeling NPs with tau antibody R2295 and APP antibody 22C11, a dystrophic neurite marker which shows that NP tau is localized in dystrophic neurites surrounding Aβ plaques. **c,** Triple-labeling NPs with AT8, NAB228 and dendritic marker MAP2, showing NPs were not localized in dendrites. **d-e,** triple-labeling NPs with AT8, NAB228 and axonal marker phospho-independent neurofilament light chain antibody NFL (**d)**, or phospho-dependent heavy and middle neurofilament chains MAb TA51 (**e)**, showing NPs are localized in axons. **f,** Triple-labeling NPs with R2295, NAB228 and presynaptic marker synaptophysin antibody, which demonstrate that NPs are localized in presynaptic dystrophic neurites. Arrows and arrow heads in **b,** and **d** to **f,** indicate the aforementioned co-localizations. **g,** Triple-labeling NPs with AT8, excitatory synaptic vesicle marker VGLUT1 antibody and inhibitory synaptic vesicle marker VGAT antibody, showing that NPs are mostly localized in dystrophic axons enriched with excitatory synaptic vesicles, but to a lesser extent also in dystrophic axons with inhibitory synaptic vesicles. The brain slices were from AD-APP KI (15mo) or AD-5xFAD (8mo) mice at 3 mo.p.i.. **a, c-g**, scale bar, 10 μm; **b**, scale bar, 10 μm.

Supplementary Fig. 7

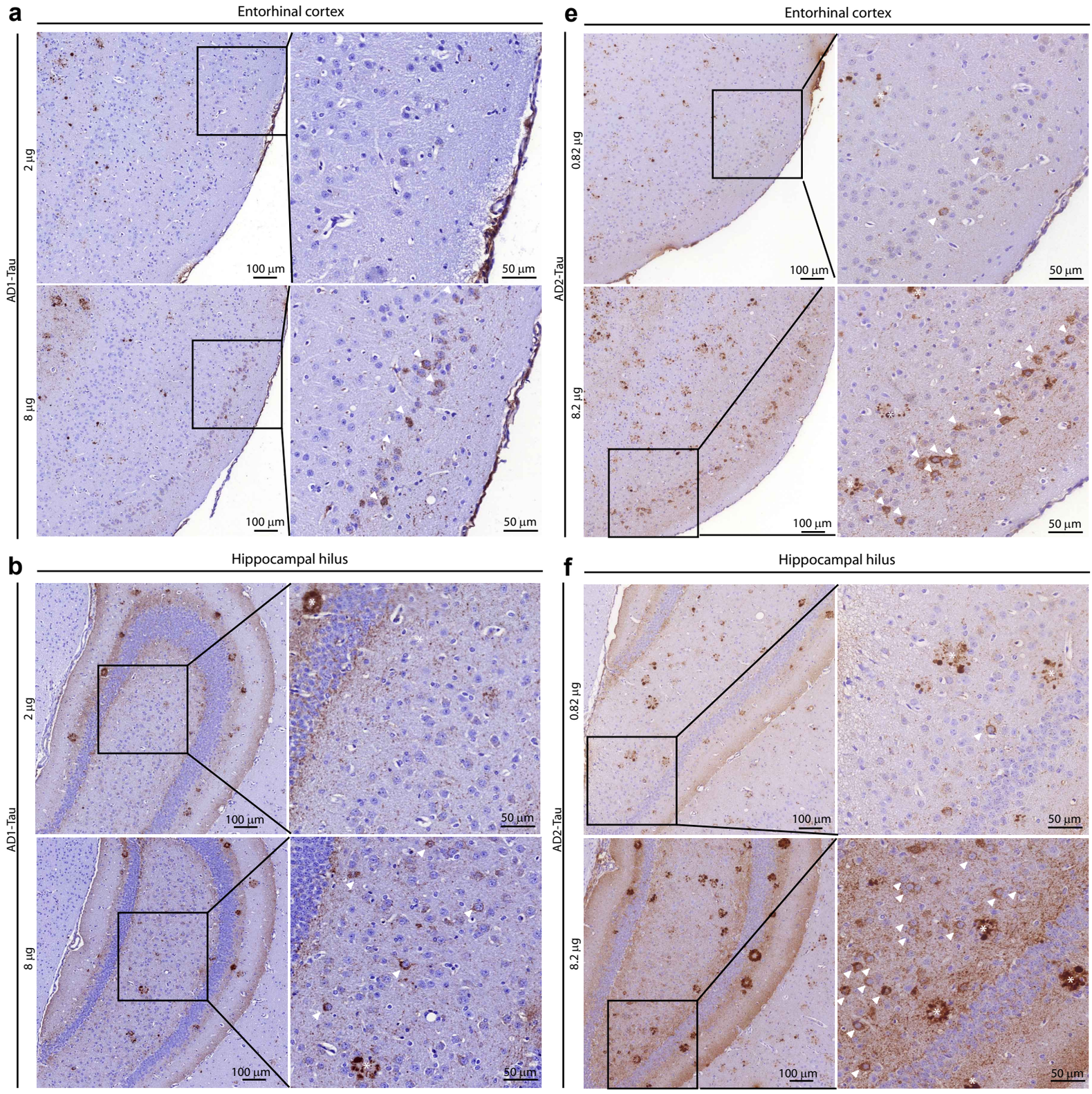

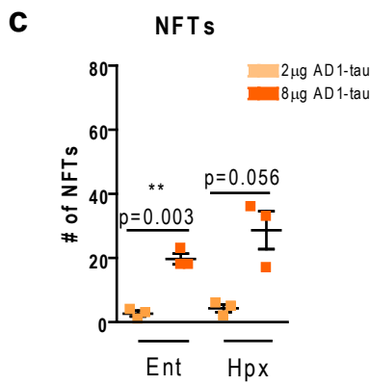

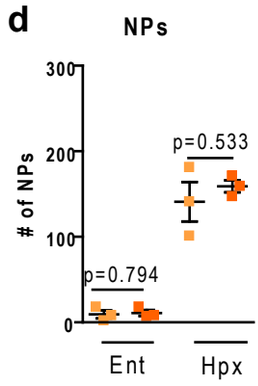

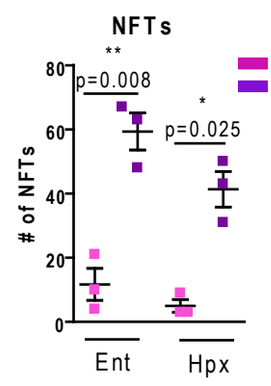

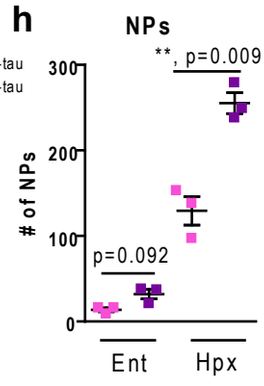

Supplementary Figure 7: High, but not low, doses of AD-tau induce significant NFTs in 5xFAD mice with abundant Aβ plaques.

5xFAD (4mo) with abundant Aβ plaques were injected with low or high dose AD-tau extracted from two different AD brains. **a-d,** AD-tau extracted from AD1 brain were injected into 5xFAD mouse brains at low or high (2 or 8 μg per mouse) doses. Representative AT8 immunostaining of ipsilateral entorhinal cortex (**a**) and ventral hippocampal hilus regions (**b**) from low doses (2 μg per mouse) or high doses (8 μg per mouse) of a AD1-tau injected 5xFAD (4mo) mice at 3 mo.p.i.. Quantification of NFTs (**c)** and NPs (**d**) in both entorhinal cortex and hippocampus on the ipsilateral side of the mice shown in **a, b**. **e-h,** AD-tau extracted from AD2 brain were injected into 5xFAD mouse brains at low or high (0.82 or 8.2 μg per mouse) dose. Representative AT8 immunostaining of ipsilateral entorhinal cortex (**e**) and ventral hippocampal hilus regions (**f**) from low doses (0.82 μg per mouse) or high doses (8.2 μg per mouse) of AD2-tau injected 5xFAD (4mo) mice at 3 mo.p.i.. Quantification of NFTs (**g)** and NPs (**h**) in both entorhinal cortex and hippocampus on the ipsilateral side of the mice shown in **e, f**. The black frames at the left indicate the higher magnification images on the right. White arrowheads indicate the NFTs, and the asterisks indicate NPs. Note that the NFTs are almost formed in the high dose AD-tau injected 5xFAD mice while the low dose AD-tau injected 5xFAD mice almost only show NPs. Three mice per group were quantified and two-tailed t-tests were performed, with *, $p \leq 0.05$; **, $p \leq 0.01$. AD-tau extracted from the AD1 case is somewhat less potent than the extracts from the AD2 case, which was derived from an old Down's Syndrome patient.

Supplementary Fig. 8

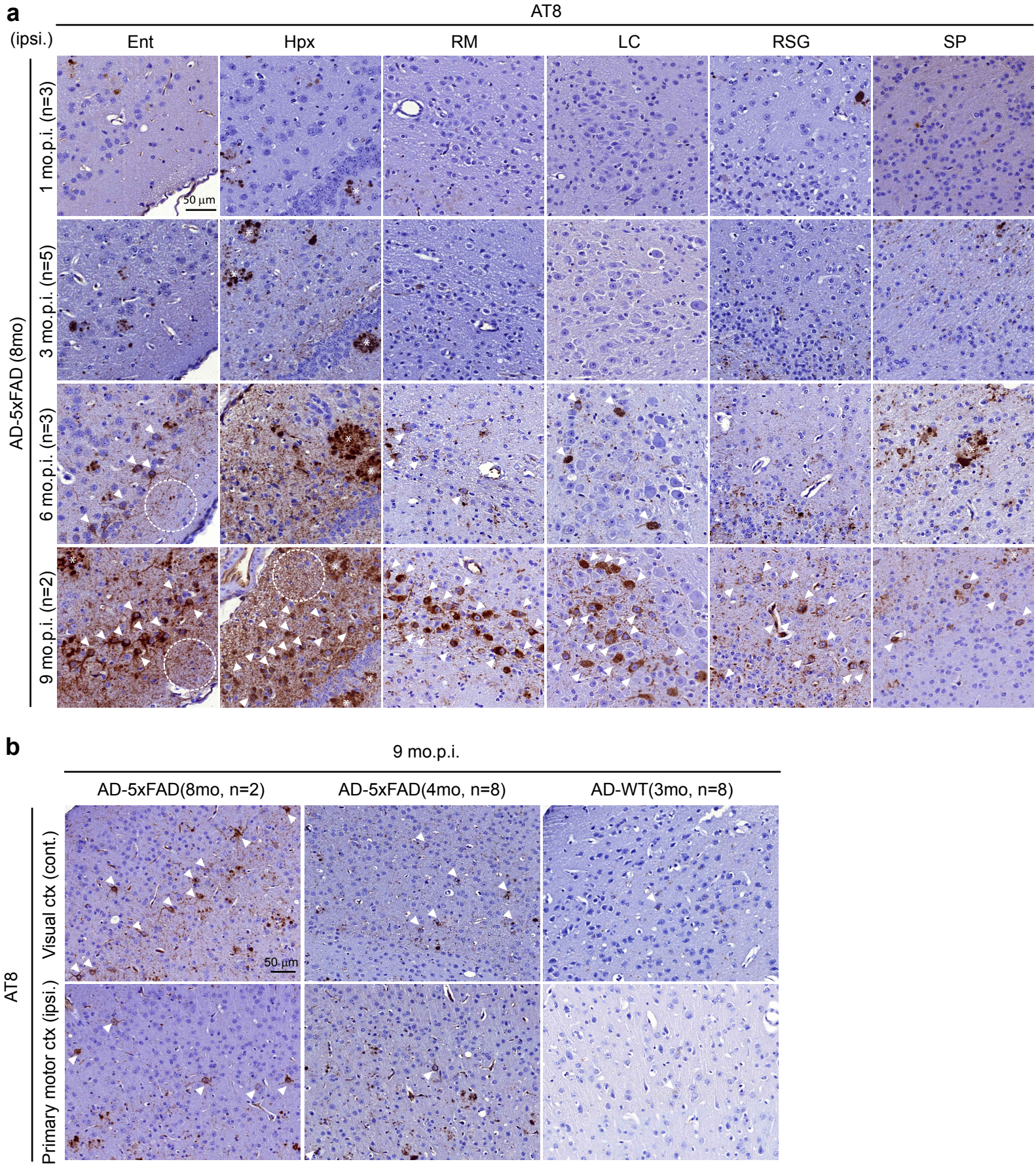

Nature Medicine: doi:10.1038/nm.4443

Supplementary Figure 8: AD-tau injected old 5xFAD mice with a high density of NPs developed abundant NFTs at later time points post-injection.

a, Representative images of tau pathologies revealed by MAb AT8 in the ipsilateral sides of AD-5xFAD (8mo) mice from 1 to 9 months after AD-tau injections. NFTs that were relatively absent before 3 mo.p.i. first appeared in entorhinal cortex at 6 mo.p.i. and spread to different brain regions at 9 mo.p.i.. **b,** AT8-labeled NFTs induced in AD-5xFAD (8mo) mice at 9 mo.p.i. spread to the ipsilateral primary motor cortex and contralateral visual cortex, where minimal NFTs were present in WT mice injected with the same amount of AD-tau after the same inoculation period. White arrowheads indicate the NFTs, dashed white circles indicate NTs, and the asterisks indicate NPs. Ent, entorhinal cortex; Hpx, hippocampus; RM, retromammillary nucleus; LC, locus coeruleus; RSG, retrosplenial granular cortex; SP, septal nucleus; ctx, cortex. 3 to 8 mice as indicated were analyzed for each time point, except only two 5xFAD (8mo) survived to 9 mo.p.i..

Supplementary Fig. 9

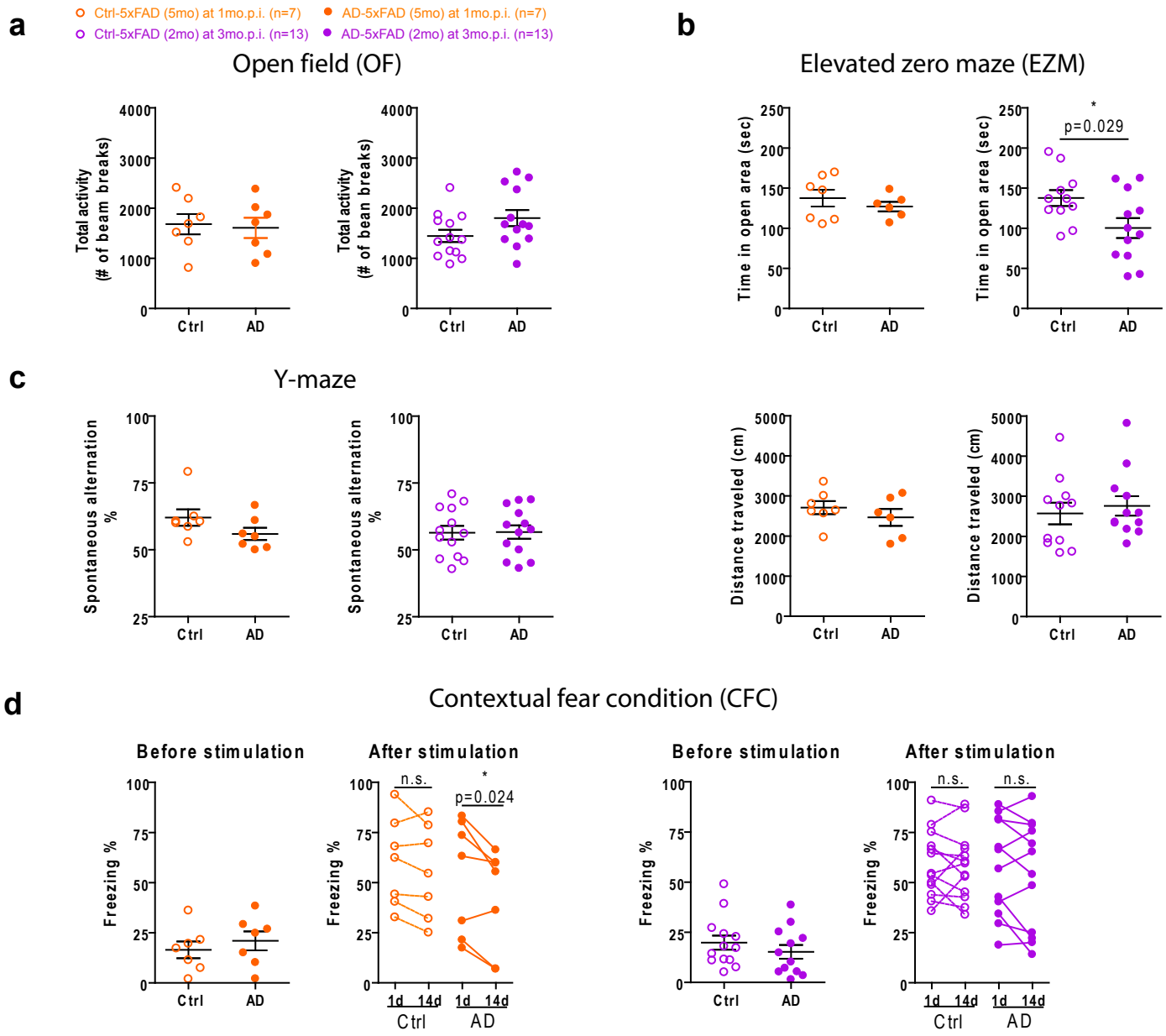

Supplementary Figure 9: Additional behavior tests conducted in mice with NPs alone, or with both NPs and NFTs

AD-5xFAD (5mo) mice after 1 mo.p.i. exclusively developed NPs while AD-5xFAD (2mo) mice after 3 mo.pi. contained both NFTs and NPs. Age-matched uninjected littermate 5xFAD mice were used as controls. **a**, Open field testing shows no locomotor deficit in all the mice. **b**, Elevated zero maze results reveal AD-5xFAD (2mo) mice at 3 mo.p.i. spent less time in the open area than the control mice, whereas AD-5xFAD (5mo) at 1 mo.p.i. did not show any difference from age-matched control mice, suggesting that the AD-5xFAD (2mo) mice but not AD-5xFAD (5mo) mice showed anxiety-related behavior. **c**, Y-maze showing that mice with either NPs or both of NFTs and NPs had normal short-term memory as revealed by spontaneous alternation. Two-tailed t-tests were used in **a-c**, with *, $p \leq 0.05$. **d**, Contextual fear conditioning testing shows that the basal freezing level before footshock stimulation was normal in both AD-5xFAD (5mo) mice at 1mo.p.i. and AD-5xFAD (2mo) mice at 3 mo.p.i. Statistical analysis was performed by a two-tailed t-test. After the footshock stimulation, AD-5xFAD (2mo) mice at 3 mo.p.i. showed similar learning trends from 1 to 14 days post-stimulation compared to control mice. However, AD-5xFAD (5mo) mice at 1 mo.p.i. showed decreased freezing levels from 1 to 14 days, while no such changes were observed in age-matched control 5xFAD mice. Statistical analysis was conducted by a two-way ANOVA with repeated measures. AD-5xFAD (5mo): time ($p=0.005$, $F=12.11$, $DF=1$), AD ($p=0.441$, $F=0.634$, $DF=1$), interaction ($p=0.188$, $F=1.949$, $DF=1$), followed by two-tailed paired t-test. Each group contains 7-13 mice and each animal is indicated by a dot in the graphs.

Supplementary Fig.10

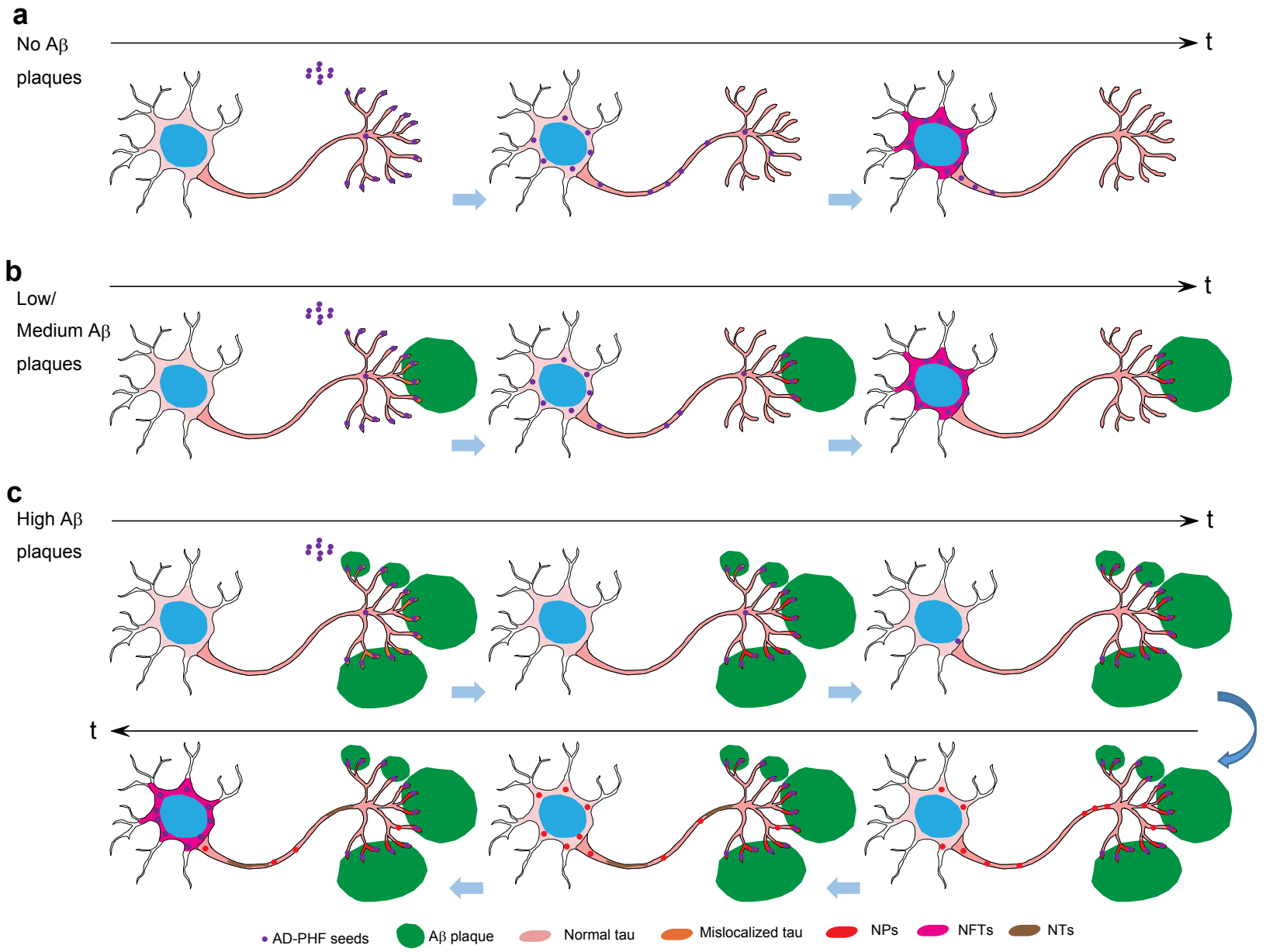

Nature Medicine: doi:10.1038/nm.4443

Supplementary Figure 10: Multi-step mechanism underlying Aβ plaque enhancement of tau seeded pathogenesis.

Schematic diagrams summarizing a hypothesized mechanism of seeded tau pathogenesis in the absence or presence of Aβ plaques. **a,** In the presence of pathological tau seeds, but in the absence of Aβ plaques, endogenous mouse tau proteins may be slowly recruited into perikaryal deposits in vulnerable neurons to form NFTs. **b**, In the presence of a low/medium Aβ plaque burden, mislocalized soluble endogenous tau accumulates in limited dystrophic neurites surrounding few Aβ plaques, and therefore provide an accessible source of substrate for tau aggregation. Once pathological tau seeds enter those limited dystrophic neurites they seed the misfolding and aggregation of the accumulated tau, forming NPs. In addition, the remaining "unutilized" pathological tau seeds could likely be transported into neuronal somas to form NFTs, albeit at a slower rate than NP formation. **c,** In the presence of abundant Aβ plaques, numerous dystrophic neurites with accumulated soluble tau are present. When pathological tau seed concentration is low, the internalized seeds are inferred to be consumed during seeding of NPs, leaving insufficient seeds to be transported to the soma to form NFTs. However, as the NP tau aggregates mature, small fragments of these aggregates could possibly break off and function as secondary pathological seeds through retrograde transport back into the parent neuronal somas, thereby seeding NT and NFT formation. Alternatively, they might also be released extracellularly and taken up by nearby dystrophic neurites around Aβ plaques to form new NPs in a relative short period of time and initiate formation of NFTs later in new cycles of pathological tau amplification, thereby leading to the progressive spread of NFTs in regions with Aβ plaques, and eventually throughout the AD brain.

Nature Medicine: doi:10.1038/nm.4443

Supplementary Fig. 11

Fig. 2b_1mo.p.i.

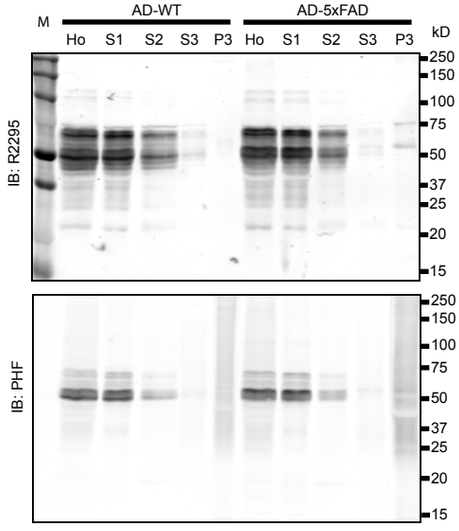

Fig. 2c_3mo.p.i.

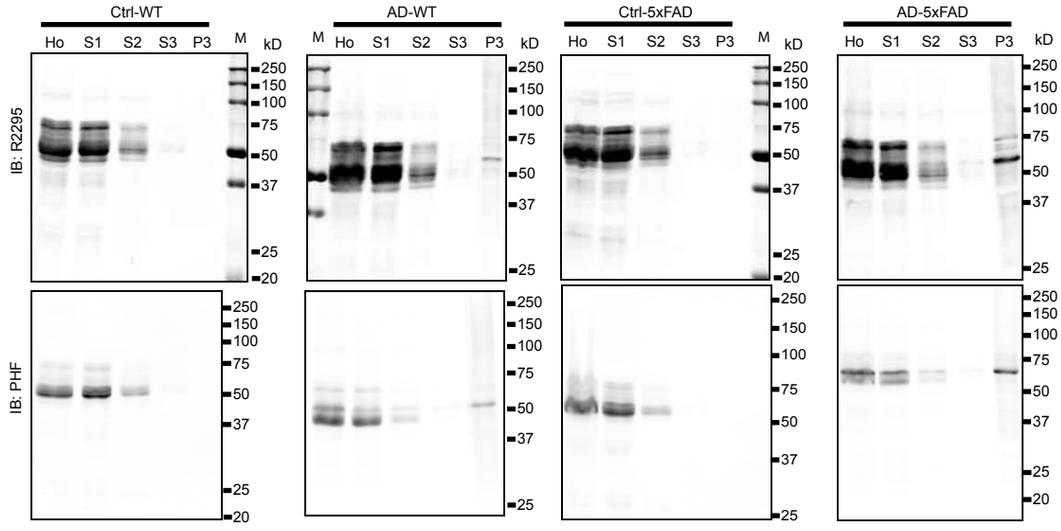

Fig. 3f

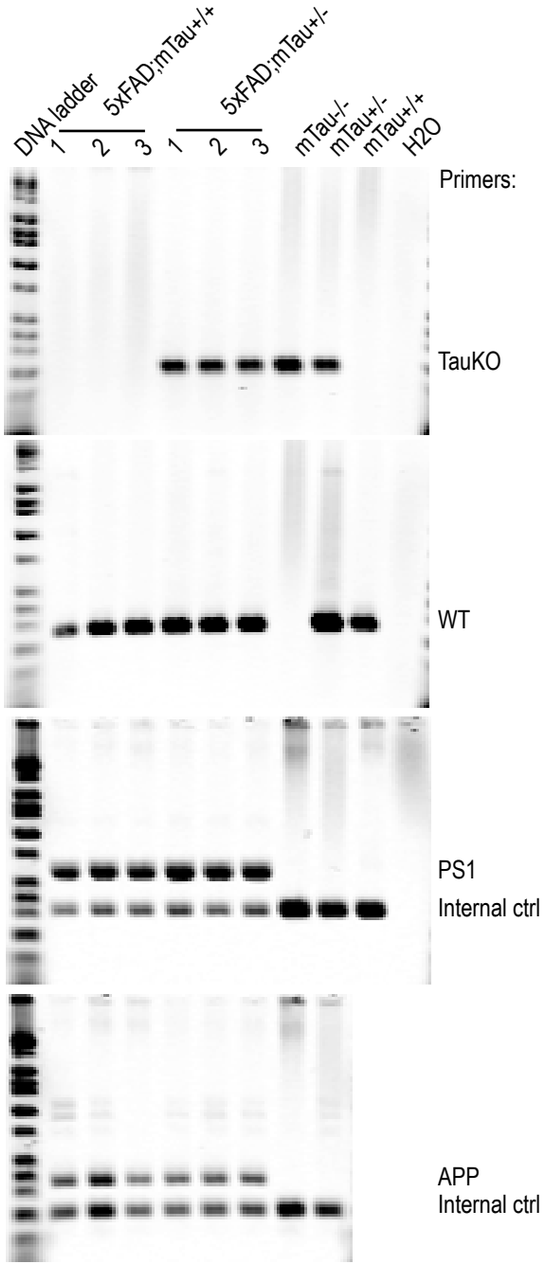

Fig. 3g

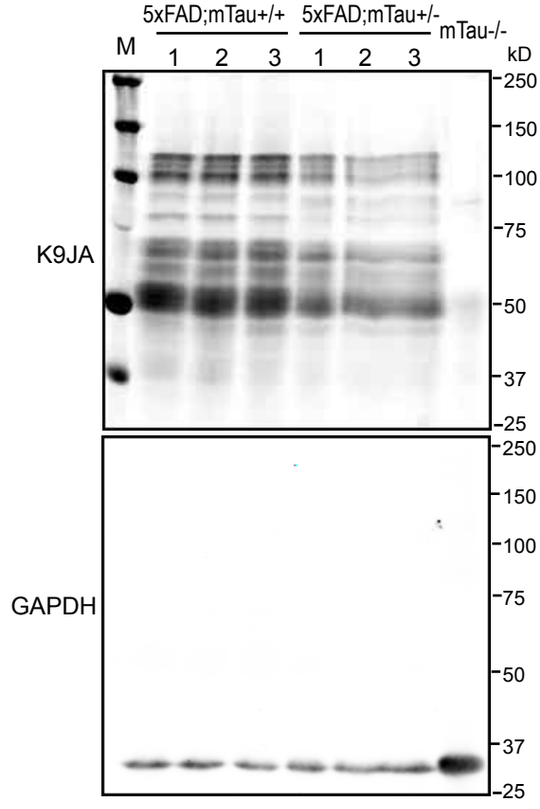

Supplementary Figure 11: Full length blots and gels for the cropped images shown in the paper.

Supplementary Table 1. Demographics of human cases used in these studies

Case No.	Neuropathological Diagnosis	Gender	Age at death	PMI (hr)
1	AD	F	68	9
2	AD	F	59	14
3	AD	M	66	4
4	AD	F	87	20
5	AD	F	73	4
6	AD	F	82	9
7	AD	F	70	6
8	AD	M	84	20
9	AD	F	67	11
10	AD	F	64	6
11	AD	M	94	16
12	AD	F	88	14
13	AD	M	86	14
14	AD	M	77	4.5
15	AD	F	89	18
16	AD	F	101	11.5
17	AD	F	75	19
18	AD	M	64	9
19	AD	F	64	20
20	AD	F	93	5
21	AD	M	91	9
22	AD	M	88	17
23	AD	F	61	24
24	AD	M	71	22
25	AD	M	54	18
26	AD	F	85	9
27	AD	F	86	6
28	AD	F	72	5
29	AD	M	85	16
30	AD	M	77	17
31	AD	F	65	8.5
32	AD	F	80	
33	AD	F	83	20
34	AD	M	71	4.5
35	AD	F	61	8
36	AD	F	85	8
37	AD	F	72	12
38	AD	M	93	5
39	AD	M	60	12
40	AD DS*	M	54	14
41	AD DS*	M	58	13

Nature Medicine: doi:10.1038/nm.4443

42	DS	F	53	15
43	DS	F	38	21
44	DS	M	33	24
45	DS	F	67	17
46	PART	M	90	6
47	PART	M	75	17
48	PART	F	82	5
49	PART	M	86	32
50	PART	M	92	6
51	PART	F	88	16
52	PART	M	67	18
53	Normal	M	59	17
54	Normal	F	75	18

*: Down Syndrome patients with postmortem neuropathological diagnosis of AD.

Nature Medicine: doi:10.1038/nm.4443

Supplementary Table 2. Antibodies used in these studies

Antibody Name	Specificity	Host Species	Dilutions	Source
R2295 mTau	mouse tau	rabbit polyclonal	1:1000 (WB, IF)	In-house
R2295 h&mTau	human and mouse tau	rabbit polyclonal	1:1000 (WB, IF)	In-house
AT8	p-tau (phosphorylated at Ser202 and Thr 205)	mouse monoclonal, IgG1	1:1000 (WB); 1:10000 (IHC); 1:2000 (IF)	Thermo Scientific
PHF-1	p-tau (phosphorylated at Ser396 and Ser404)	mouse monoclonal, IgG1	1:1000 (WB)	Gift from Dr. Peter Davies
AT180	p-tau (phosphorylated at Thr 231)	mouse monoclonal, IgG1	1:1000 (IHC)	Thermo Scientific
12E8	p-tau (phosphorylated at pSer262/pSer356)	mouse monoclonal, IgG1	1:5000 (IHC)	In-house
pSer422	p-tau (phosphorylated at pSer422)	mouse monoclonal	1:1000 (IHC)	Gift from Dr. Michel Goedert
T46	tau (aa 401-441)	mouse monoclonal, IgG1	1:1000 (WB)	In-house
K9JA	tau (aa 243-441)	rabbit polyclonal	1:5000 (WB); 1:200 (IF)	Dako
Anti-4R tau	4R tau	rabbit polyclonal	1:2000 (WB)	Cosmo Bio USA
MC1	tau in the pathological conformation	mouse monoclonal, IgG1	1:250 (WB); 1:5000 (IHC)	Gift from Dr. Peter Davies
Alz50	tau in the pathological conformation	mouse monoclonal, IgM	1:500 (IHC)	Gift from Dr. Peter Davies
TG3	Epitope around Thr231, in the pathological conformation	mouse monoclonal, IgM	1:100 with citrate buffer boil (IF)	Gift from Dr. Peter Davies
TOC1	Oligomeric tau	mouse monoclonal, IgM	1:3000 with citrate buffer boil (IF)	Gift from Dr. Lester Binder
HT7	human tau (aa 159-163)	mouse monoclonal, IgG1	1:500 (IF)	Pierce
Biotinylated BT2	tau (aa 194-198)	mouse monoclonal	31.25 ng/ml as reporting antibody in tau ELISA	Pierce

Nature Medicine: doi:10.1038/nm.4443

			together with HT7	
Biotinylated HT7	tau (aa 159-163)	mouse monoclonal	62.5 ng/ml as reporting antibody in tau ELISA together with BT2	Pierce
17028	MAP2	rabbit polyclonal	1:2000 (IF)	In-house
NFL	Phospho-independent neurofilament light chain	rabbit polyclonal	1:1000 (IF)	In-house
TA51	Phospho-dependent neurofilament heavy and middle chain	rat monoclonal	1:25 (IF)	In-house
Synaptophysin	Synaptophysin	mouse monoclonal, IgG1	1:200 (IF)	Millipore
VGLUT1	Vesicular glutamate transporter 1	Guinea pig	1:1000 (IF)	Synaptic System
VGAT	Vesicular GABA Transporter	rabbit polyclonal	1:1000 (IF)	Synaptic System
β-actin	actin	mouse monoclonal, IgM	1:200 (IF)	ProteinTech Group
22C11	hAPP (aa 66-81)	mouse monoclonal, IgG1	1:250 (IF)	Millipore
Ubiquitin	Ubiquitin	rabbit polyclonal	1:500 (IF)	Dako
P62	P62	mouse monoclonal, IgG2a	1:500 (IF)	Abnova
2.2B10	GFAP	rat monoclonal	1:1000 (IF)	In-house
Iba1	Iba1	rabbit polyclonal	1:1000 (IF)	Wako
NeuN	NeuN	mouse monoclonal, IgG1	1:500 (IHC)	Millipore
9027	α-syn (aa 130-140)	mouse monoclonal	3.3 μg/ml as capture antibody for α-syn ELISA	In-house
MJF-R1	α-syn (aa 118-123)	rabbit monoclonal	0.5425 μg/ml as reporting antibody for α-syn ELISA	Abcam
Ban50	Aβ (aa 1-10)	mouse monoclonal	10 μg/ml as capture antibody for Aβ1-40 and 1-42 ELISA	Takeda Pharmaceutical
NAB228	Aβ (aa 1-11)	mouse monoclonal, IgG2a	1:1000 (IHC); 1:1000 (IF0	In-house
BA27	Aβ1-40	mouse monoclonal, IgG2a	1:10000 (IHC)	Takeda Pharmaceutical

Nature Medicine: doi:10.1038/nm.4443

HRP-labeled BA27	Aβ1-40	mouse monoclonal	reporting antibody for Aβ1-40 ELISA (concentration not determined after HRP labeling)	Takeda Pharmaceutical
HRP-labeled BC05	Aβ1-42	mouse monoclonal	reporting antibody for Aβ1-42 ELISA (concentration not determined after HRP labeling)	Takeda Pharmaceutical

Abbreviations: WB - western blotting; IHC -immunohistochemistry; IF – immunofluorescence.

Nature Medicine: doi:10.1038/nm.4443

Supplementary Table 3: **Detailed information for statistical analysis.**

Fig. #	Compare (group size n=)	Statistical method	P value	t value	F value	Degrees of freedom
Fig. 1o	AT8+ NFT number in ipsilateral hippocampus of different AD-mice at 3 mo.p.i..	One-way ANOVA, with Tukey's multiple comparison test	<0.0001		88.47	25
	WT(15mo, n=5) vs APP KI(6mo, n=3)		>0.05			
	WT(15mo, n=5) vs APP KI(15mo, n=5)		>0.05			
	WT(15mo, n=5) vs 5xFAD(2mo, n=8)		<0.001			
	WT(15mo, n=5) vs 5xFAD(8mo, n=5)		<0.001			
	APP KI(6mo, n=3) vs APP KI(15mo, n=5)		>0.05			
	APP KI(6mo, n=3) vs 5xFAD(2mo, n=8)		<0.001			
	APP KI(6mo, n=3) vs 5xFAD(8mo, n=5)		<0.001			
	APP KI(15mo, n=5) vs 5xFAD(2mo, n=8)		<0.001			
	APP KI(15mo, n=5) vs 5xFAD(8mo, n=5)		<0.001			
	5xFAD(2mo, n=8) vs 5xFAD(8mo, n=5)		<0.001			
Fig. 1p	AT8+ NP number in ipsilateral hippocampus of different AD-mice at 3 mo.p.i..	One-way ANOVA, with Tukey's multiple comparison test	<0.0001		336.9	25
	WT(15mo, n=5) vs APP KI(6mo, n=3)		>0.05			
	WT(15mo, n=5) vs APP KI(15mo, n=5)		>0.05			
	WT(15mo, n=5) vs 5xFAD(2mo, n=8)		<0.001			
	WT(15mo, n=5) vs 5xFAD(8mo, n=5)		<0.001			
	APP KI(6mo, n=3) vs APP KI(15mo, n=5)		>0.05			
	APP KI(6mo, n=3) vs 5xFAD(2mo, n=8)		<0.001			
	APP KI(6mo, n=3) vs 5xFAD(8mo, n=5)		<0.001			

Nature Medicine: doi:10.1038/nm.4443

	APP KI(15mo, n=5) vs 5xFAD(2mo, n=8)		<0.001			
	APP KI(15mo, n=5) vs 5xFAD(8mo, n=5)		<0.001			
	5xFAD(2mo, n=8) vs 5xFAD(8mo, n=5)		<0.001			
Fig. 1q	AT8+ NP number vs Aβ burden	Spearman Rank-Order Correlation Coefficient	<0.001	12.83		24
Fig. 1r	AT8+ NFT number in ipsilateral Entorhinal cortex of different AD-mice at 3 mo.p.i..	One-way ANOVA, with Tukey's multiple comparison test	<0.0001		37.45	25
	WT(15mo, n=5) vs APP KI(6mo, n=3)		>0.05			
	WT(15mo, n=5) vs APP KI(15mo, n=5)		<0.001			
	WT(15mo, n=5) vs 5xFAD(2mo, n=8)		<0.001			
	WT(15mo, n=5) vs 5xFAD(8mo, n=5)		<0.001			
	APP KI(6mo, n=3) vs APP KI(15mo, n=5)		<0.001			
	APP KI(6mo, n=3) vs 5xFAD(2mo, n=8)		<0.001			
	APP KI(6mo, n=3) vs 5xFAD(8mo, n=5)		<0.001			
	APP KI(15mo, n=5) vs 5xFAD(2mo, n=8)		>0.05			
	APP KI(15mo, n=5) vs 5xFAD(8mo, n=5)		>0.05			
	5xFAD(2mo, n=8) vs 5xFAD(8mo, n=5)		>0.05			
Fig. 1s	AT8+ NP number in Hpx vs AT8+ NFT number in Ent	Spearman Rank-Order Correlation Coefficient	<0.001	-9.68		24
Fig. 2d	R2295 O.D. in insoluble fraction from AD-WT (n=3) v.s. AD-5xFAD (n=3) at 1mo.p.i.	2-sided, unpaired t-test	0.034		3.166	4
Fig. 2e	PHF-1 O.D. in insoluble fraction from AD-WT (n=3) v.s. AD-5xFAD (n=3) at 1mo.p.i.	2-sided, unpaired t-test	0.0676		2.488	4
Fig. 2f	R2295 O.D. in insoluble fraction from AD-WT (n=5) v.s. AD-5xFAD (n=4) at 3mo.p.i.	2-sided, unpaired t-test	0.0099		3.505	7
Fig. 2g	PHF-1 O.D. in insoluble fraction from AD-WT (n=5) v.s. AD-5xFAD (n=4) at 3mo.p.i.	2-sided, unpaired t-test	0.0078		3.687	7

Nature Medicine: doi:10.1038/nm.4443

Fig. 3b	Compact plaque fraction in Ctrl-(n=3) v.s. AD-5xFAD (n=3)	2-sided, unpaired t-test, Welch-corrected	0.1669	2.13		2
Fig. 3c	Non-compact v.s. compact Aβ plaques with K9JA+ accumulated tau (n=3)	2-sided, paired t-test	0.0449	4.559		2
Fig. 3e	Non-compact v.s. compact Aβ plaques with AT8+ NP tau (n=3)	2-sided, paired t-test	0.0341	5.273		2
Fig. 3i	NAB228 area% in 5xFAD;mTau+/+ (n=3) v.s. AD-5xFAD;mTau+/- (n=3)	2-sided, unpaired t-test, Welch-corrected	0.2503	1.602		2
Fig. 3k	Hippocampal NP number in AD-5xFAD;mTau+/+ (n=3) v.s. AD-5xFAD;mTau+/- (n=3)	2-sided, unpaired t-test, Welch-corrected	0.0165	4.875		3
	Cortical NP number in AD-5xFAD;mTau+/+ v.s. AD-5xFAD;mTau+/-	2-sided, unpaired t-test, Welch-corrected	0.0158	4.951		3
Fig. 3l	AT8+ area% in each NP in AD-5xFAD;mTau+/+ (n=235) v.s. AD-5xFAD;mTau+/- (n=121)	2-sided, unpaired t-test	<0.0001	12.47		354
Fig. 4c	NT in AD-5xFAD at 3mo.p.i. F(n=3) v.s. 9mo.p.i. (n-8) in Hip. DG	2-sided, unpaired t-test, Welch-corrected	0.0021	4.760		7
Fig. 4d	AT8+ NFTs in the Ent regions of 3mo.p.i. AD-5xFAD(n=3), 9mo.p.i. AD-5xFAD(n=8), 6mo.p.i. AD-WT(n=4) and 9mo.p.i. AD-5xFAD(n=8)	One-way ANOVA, with Tukey's multiple comparison test	<0.0001		21.96	22
	AT8+ NFTs in the Hpx regions of 3mo.p.i. AD-5xFAD(n=3), 9mo.p.i. AD-5xFAD(n=8), 6mo.p.i. AD-WT(n=4) and 9mo.p.i. AD-5xFAD(n=8)	One-way ANOVA, with Tukey's multiple comparison test	0.0016		7.570	22
Fig. 4e	MC1+ NFT in AD-WT(n=8) v.s. AD-5xFAD(n=8) in Ent	2-sided, unpaired t-test, Welch-corrected	0.0032	3.667		12
	MC1+ NFT in AD-WT(n=8) v.s. AD-5xFAD(n=8) in Hpx	2-sided, unpaired t-test, Welch-corrected	0.0546	2.112		13
Fig. 4f	ThioS+ NFT in AD-WT(n=8) v.s. AD-5xFAD(n=8) in Ent	2-sided, unpaired t-test, Welch-corrected	0.0008	4.343		13
	ThioS+ NFT in AD-WT(n=8) v.s. AD-5xFAD(n=8) in Hpx	2-sided, unpaired t-test, Welch-corrected	<0.0001	6.252		12

Nature Medicine: doi:10.1038/nm.4443

Fig. 5b	Early AD_Sup. Temp. (n=16) NPs v.s. NFTs	2-sided, paired t-test	0.1359	1.576		15
Fig. 5c	Early AD_Visual (n=16) NPs v.s. NFTs	2-sided, paired t-test	0.0306	2.516		10
Fig. 5d	Late AD_Sup. Temp. (n=16) NPs v.s. NFTs	2-sided, paired t-test	0.2064	1.321		15
Fig. 5e	Late AD_Visual (n=17) NPs v.s. NFTs	2-sided, paired t-test	<0.0001	6.286		16
Fig. 6b	Total activity Ctrl (n=13) v.s. AD-WT (n=10)	2-sided, unpaired t-test, Welch-corrected	0.6636	0.4418		19
	Total activity Ctrl (n=8) v.s. AD-5xFAD (n=10)	2-sided, unpaired t-test, Welch-corrected	0.4925	0.7063		13
Fig. 6c	Open area Ctrl (n=13) v.s. AD-WT (n=10)	2-sided, unpaired t-test, Welch-corrected	0.0178	2.582		20
	Total distance Ctrl (n=13) v.s. AD-WT (n=10)	2-sided, unpaired t-test, Welch-corrected	0.0939	1.763		19
	Open area Ctrl (n=7) v.s. AD-5xFAD (n=10)	2-sided, unpaired t-test, Welch-corrected	0.5845	0.5634		11
	Total distance Ctrl (n=7) v.s. AD-5xFAD (n=10)	2-sided, unpaired t-test, Welch-corrected	0.2987	1.079		10
Fig. 6d	Y-maze spontaneous alternation Ctrl (n=12) v.s. AD-WT (n=10)	2-sided, unpaired t-test, Welch-corrected	0.4484	0.7741		19
	Y-maze spontaneous alternation Ctrl (n=8) v.s. AD-5xFAD (n=10)	2-sided, unpaired t-test, Welch-corrected	0.5489	0.6133		15
Fig. 6e	Before stimulation Ctrl (n=13) v.s. AD-WT (n=10)	2-sided, unpaired t-test, Welch-corrected	0.0226	2.586		13
	After stimulation Ctrl (n=13) v.s. AD-WT (n=10)	Two-way ANOVA with repeated measurements	Interaction=0.2131; Time=0.7050; AD=0.8133		Interaction=1.649; Time=0.1473; AD=0.05718	Interaction=1; Time=1; AD=1
	Before stimulation Ctrl (n=8) v.s. AD-5xFAD (n=10)	2-sided, unpaired t-test, Welch-corrected	0.7666	0.3051		10

Nature Medicine: doi:10.1038/nm.4443

	After stimulation Ctrl (n=8) v.s. AD-5xFAD (n=10)	Two-way ANOVA with repeated measurements	Interaction=0.0612; Time=0.0466; AD=0.6176		Interaction=4.054; Time=4.649; AD=0.2592	Interaction=1; Time=1; AD=1
	After stimulation Ctrl 5xFAD (n=8) 1d v.s. 14d	2-sided, paired t-test	0.8674	0.1731		8
	After stimulation AD-5xFAD (n=10) 1d v.s. 14d	2-sided, paired t-test	0.0328	2.52		9
Fig. 6h	WT (n=6) v.s. AD-WT (n=6)	Two-way ANOVA with repeated measurements	Interaction=0.9635; Region<0.0001; AD=0.0045		Interaction=0.0373; Region=29.93; AD=11.17	Interaction=2; Region=2; AD=1
	WT (n=6) v.s. AD-WT (n=6) in DG	2-sided, unpaired t-test, Welch-corrected	0.2196	1.32		9
	WT (n=6) v.s. AD-WT (n=6) in Hilus	2-sided, unpaired t-test, Welch-corrected	0.0942	1.899		8
	WT (n=6) v.s. AD-WT (n=6) in CA3	2-sided, unpaired t-test, Welch-corrected	0.0327	2.579		8
	5xFAD (n=3) v.s. AD-5xFAD (n=3)	Two-way ANOVA with repeated measurements	Interaction=0.9555; Region=0.0134; AD=0.3621		Interaction=0.0459; Region=9.644; AD=0.9727	Interaction=2; Region=2; AD=1
S. Fig. 1d	AT180+ NFT number in ipsilateral hippocampus of different AD-mice at 3 mo.p.i..	One-way ANOVA, with Tukey's multiple comparison test	<0.0001		28.48	25

Nature Medicine: doi:10.1038/nm.4443

	WT(15mo, n=5) vs APP KI(6mo, n=3)		>0.05			
	WT(15mo, n=5) vs APP KI(15mo, n=5)		>0.05			
	WT(15mo, n=5) vs 5xFAD(2mo, n=8)		<0.001			
	WT(15mo, n=5) vs 5xFAD(8mo, n=5)		<0.001			
	APP KI(6mo, n=3) vs APP KI(15mo, n=5)		>0.05			
	APP KI(6mo, n=3) vs 5xFAD(2mo, n=8)		<0.001			
	APP KI(6mo, n=3) vs 5xFAD(8mo, n=5)		<0.001			
	APP KI(15mo, n=5) vs 5xFAD(2mo, n=8)		<0.001			
	APP KI(15mo, n=5) vs 5xFAD(8mo, n=5)		<0.001			
	5xFAD(2mo, n=8) vs 5xFAD(8mo, n=5)		>0.05			
S. Fig. 1e	AT180+ NP number in ipsilateral hippocampus of different AD-mice at 3 mo.p.i..	One-way ANOVA, with Tukey's multiple comparison test	<0.0001		46.12	25
	WT(15mo, n=5) vs APP KI(6mo, n=3)		>0.05			
	WT(15mo, n=5) vs APP KI(15mo, n=5)		>0.05			
	WT(15mo, n=5) vs 5xFAD(2mo, n=8)		<0.001			
	WT(15mo, n=5) vs 5xFAD(8mo, n=5)		<0.001			
	APP KI(6mo, n=3) vs APP KI(15mo, n=5)		>0.05			
	APP KI(6mo, n=3) vs 5xFAD(2mo, n=8)		<0.01			
	APP KI(6mo, n=3) vs 5xFAD(8mo, n=5)		<0.001			
	APP KI(15mo, n=5) vs 5xFAD(2mo, n=8)		>0.05			
	APP KI(15mo, n=5) vs 5xFAD(8mo, n=5)		<0.001			

Nature Medicine: doi:10.1038/nm.4443

	5xFAD(2mo, n=8) vs 5xFAD(8mo, n=5)		<0.001			
S. Fig. 1f	AT180+ NFT number in ipsilateral Entorhinal cortex of different AD-mice at 3 mo.p.i..	One-way ANOVA, with Tukey's multiple comparison test	0.0013		6.649	25
	WT(15mo, n=5) vs APP KI(6mo, n=3)		>0.05			
	WT(15mo, n=5) vs APP KI(15mo, n=5)		>0.05			
	WT(15mo, n=5) vs 5xFAD(2mo, n=8)		<0.05			
	WT(15mo, n=5) vs 5xFAD(8mo, n=5)		<0.01			
	APP KI(6mo, n=3) vs APP KI(15mo, n=5)		>0.05			
	APP KI(6mo, n=3) vs 5xFAD(2mo, n=8)		>0.05			
	APP KI(6mo, n=3) vs 5xFAD(8mo, n=5)		<0.05			
	APP KI(15mo, n=5) vs 5xFAD(2mo, n=8)		>0.05			
	APP KI(15mo, n=5) vs 5xFAD(8mo, n=5)		>0.05			
	5xFAD(2mo, n=8) vs 5xFAD(8mo, n=5)		>0.05			
S. Fig. 1g	AT180+ NP number in Hpx vs AT180+ NFT number in Ent	Spearman Rank-Order Correlation Coefficient	<0.001	-6.67		24
S. Fig. 5b	NFT number in ipsilateral hippocampus of different AD-mice.	One-way ANOVA, with Tukey's multiple comparison test	<0.0001		205.4	32
S. Fig. 5c	NP number in ipsilateral hippocampus of different AD-mice.	One-way ANOVA, with Tukey's multiple comparison test	<0.0001		366.8	32
S. Fig. 5d	NFT number in ipsilateral Entorhinal cortex of different AD-mice.	One-way ANOVA, with Tukey's multiple comparison test	<0.0001		23.10	32
S. Fig. 5e	NP number in ipsilateral Entorhinal cortex of different AD-mice.	One-way ANOVA, with Tukey's multiple comparison test	<0.0001		13.24	32
S. Fig. 7c	NFTs in Ent of the mice injected with AD1-tau 2μg dose (n=3) v.s. 8μg dose (n=3)	2-sided, unpaired t-test, Welch-corrected	0.0029	9.016		3

Nature Medicine: doi:10.1038/nm.4443

	NFTs in Hpx of the mice injected with AD1-tau 2μg dose (n=3) v.s. 8μg dose (n=3)	2-sided, unpaired t-test, Welch-corrected	0.0561	4.043		2
S. Fig. 7d	NPs in Ent of the mice injected with AD1-tau 2μg dose (n=3) v.s. 8μg dose (n=3)	2-sided, unpaired t-test, Welch-corrected	0.7939	0.2854		3
	NPs in Hpx of the mice injected with AD1-tau 2μg dose (n=3) v.s. 8μg dose (n=3)	2-sided, unpaired t-test, Welch-corrected	0.5332	0.7466		2
S. Fig. 7g	NFTs in Ent of the mice injected with AD2-tau 0.82μg dose (n=3) v.s. 8.2μg dose (n=3)	2-sided, unpaired t-test, Welch-corrected	0.0083	6.247		3
	NFTs in Hpx of the mice injected with AD2-tau 0.82μg dose (n=3) v.s. 8.2μg dose (n=3)	2-sided, unpaired t-test, Welch-corrected	0.0253	6.161		2
S. Fig. 7h	NPs in Ent of the mice injected with AD2-tau 0.82μg dose (n=3) v.s. 8.2μg dose (n=3)	2-sided, unpaired t-test, Welch-corrected	0.0920	3.065		2
	NPs in Hpx of the mice injected with AD2-tau 0.82μg dose (n=3) v.s. 8.2μg dose (n=3)	2-sided, unpaired t-test, Welch-corrected	0.0090	6.072		3
S. Fig. 9a	Total activity Ctrl (n=7) v.s. AD-5xFAD(5mo) (n=7) at 1mo.p.i.	2-sided, unpaired t-test, Welch-corrected	0.8032	0.2552		11
	Total activity Ctrl (n=13) v.s. AD-5xFAD(2mo) (n=13) at 3mo.p.i.	2-sided, unpaired t-test, Welch-corrected	0.0892	1.778		22
S. Fig. 9b	Y-maze spontaneous alternation Ctrl (n=7) v.s. AD-5xFAD(5mo) (n=7) at 1mo.p.i.	2-sided, unpaired t-test, Welch-corrected	0.1379	1.6		11
	Y-maze spontaneous alternation Ctrl (n=13) v.s. AD-5xFAD (2mo) (n=13) at 3mo.p.i.	2-sided, unpaired t-test, Welch-corrected	0.943	0.07228		23
S. Fig. 9c	Open area Ctrl (n=7) v.s. AD-5xFAD(5mo) (n=6) at 1mo.p.i.	2-sided, unpaired t-test, Welch-corrected	0.4031	0.8773		9
	Total distance Ctrl (n=7) v.s. AD-5xFAD(5mo) (n=6) at 1mo.p.i.	2-sided, unpaired t-test, Welch-corrected	0.3825	0.9182		9
	Open area Ctrl (n=11) v.s. AD-5xFAD(2mo) (n=12) at 3mo.p.i.	2-sided, unpaired t-test, Welch-corrected	0.029	2.352		20
	Total distance Ctrl (n=11) v.s. AD-5xFAD(2mo) (n=12) at 3mo.p.i.	2-sided, unpaired t-test, Welch-corrected	0.6071	0.5225		20

Nature Medicine: doi:10.1038/nm.4443

S. Fig. 9d	Before stimulation Ctrl (n=13) v.s. AD-5xFAD(2mo) (n=12) at 3mo.p.i.	2-sided, unpaired t-test, Welch-corrected	0.3593	0.9364		22
	After stimulation Ctrl (n=13) v.s. AD-5xFAD(2mo) (n=12) at 3mo.p.i.	Two-way ANOVA with repeated measurement	Interaction=0.4820; Time=0.2782; AD=0.7176		Interaction=0.5107; Time=1.234; AD=0.1341	Interaction=1; Time=1; AD=1
	Before stimulation Ctrl (n=7) v.s. AD-5xFAD(5mo) (n=7) at 1mo.p.i.	2-sided, unpaired t-test, Welch-corrected	0.4905		0.7134	11
	After stimulation Ctrl (n=7) v.s. AD-5xFAD(5mo) (n=7) at 1mo.p.i.	Two-way ANOVA with repeated measurement	Interaction=0.1880; Time=0.0045; AD=0.4414		Interaction=1.919; Time=12.11; AD=0.6338	Interaction=1; Time=1; AD=1
	After stimulation Ctrl 5xFAD(2mo) (n=7) 1d v.s. 14d	2-sided, paired t-test	0.126	1.777		6
	After stimulation AD-5xFAD(5mo) (n=7) 1d v.s. 14d	2-sided, paired t-test	0.0237	3.011		6

Nature Medicine: doi:10.1038/nm.4443